N_2 and CO both occur in the same velocity component, that the velocity separation in O I and H_2 agree, and that the CO component is aligned in velocity with the higher-velocity O I component strongly supports our claim of the first detection of interstellar N_2. Our N_2 detection is further supported by the fact that the excitation temperatures of H_2 (1–0) and of N_2 agree for the longer-wavelength component. Although the N_2 *b*-value is not reliably determined, we use the S I *b*-value to improve our estimate and find $N(N_2) = (4.6 \pm 0.8) \times 10^{13}\,cm^{-2}$. We note that S I may be more extended than CO or N_2 in interstellar space. Because nitrogen has a lower cosmic abundance compared to either carbon or oxygen, we believe that $N(N_2)$ should not be larger than N(CO) and should the true N_2 *b*-value be much smaller than that for S I (although this is unlikely), significant amounts of N_2 (that is, $N(N_2) > 10^{14}\,cm^{-2}$) could be present. Our firm lower limit to $N(N_2)$ is not sensitive to the *b*-value or the choice of stellar model used to represent the stellar continuum. Taken together, these data strongly indicate that N_2 has been detected for the first time in the interstellar medium and with a column density of $N(N_2) > 3.8 \times 10^{13}\,cm^{-2}$.

From our analysis of the O I line at 1,356 Å, we find $N(O\,I) = (6.77 \pm 0.50) \times 10^{17}\,cm^{-2}$ for the component near 3 km s^{-1}. Using the observed $N(O\,I)/N(H_{tot})$ ratio $(4.74 \pm 0.81) \times 10^{-4}$ (ref. 11), this component contains $N(H_{tot}) = 1.5 \times 10^{21}\,cm^{-2}$, where $N(H_{tot}) = N(H\,I) + 2N(H_2)$. The amount of interstellar reddening for this component can be determined from the dust-to-gas ratio[28], which yields $E(B–V) = 0.26\,mag^{-1}$. Assuming that the ratio of total to selective extinction is 3.1 (ref. 29), we find that the total visual extinction is 0.8 mag. When we compare our results to models of interstellar gas-phase chemistry[1], none of the standard cloud models explain our observations. The observed N_2 fractional abundance is more than two orders of magnitude too low for dense cloud models and approximately two orders of magnitude larger than expected from models of diffuse clouds. The fact that N I shows a deficiency in its relative abundance for lines of sight with $N(H_{tot}) > 10^{21}\,cm^{-2}$ would argue that dense cloud chemistry should be important for interstellar nitrogen. However, the measured N_2 abundance and upper limits for other sightlines[7] do not account for the observed variations. Additionally, we find that the fractional abundance of N_2 towards HD 124314 is $N_2/H_2 = 3.3 \times 10^{-7}$, similar to those estimated from N_2H^+ observations[4] of dark molecular clouds. Therefore, the far-ultraviolet lines of N_2 provide a unique probe of interstellar nitrogen chemistry in the transition region from diffuse to dense molecular gas. □

Received 16 February; accepted 30 April 2004; doi:10.1038/nature02614.

1. Viala, Y. P. Chemical equilibrium from diffuse to dense interstellar clouds. I Galactic molecular clouds. *Astron. Astrophys.* (Suppl.) **64,** 391–437 (1986).
2. Bergin, E. A., Langer, W. D. & Goldsmith, P. F. Gas-phase chemistry in dense interstellar clouds including grain surface molecular depletion and desorption. *Astrophys. J.* **441,** 222–243 (1995).
3. Womack, M., Ziruys, L. M. & Wyckoff, S. A survey of N_2H^+ in dense clouds: Implications for interstellar nitrogen and ion-molecule chemistry. *Astrophys. J.* **387,** 417–429 (1992).
4. Womack, M., Ziruys, L. M. & Wyckoff, S. Estimates of N_2 abundances in dense molecular clouds. *Astrophys. J.* **393,** 188–192 (1992).
5. Lutz, B. L., Owen, T. & Snow, T. P. Jr A search with *Copernicus* for interstellar N_2 in diffuse clouds. *Astrophys. J.* **227,** 159–162 (1979).
6. Sandford, S. A., Bernstein, M. P., Allamandola, L. J., Goorvitch, D. & Teixeira, T. C. V. S. The abundances of solid N_2 and gaseous CO_2 in interstellar dense molecular clouds. *Astrophys. J.* **548,** 836–851 (2001).
7. Knauth, D. C., Andersson, B.-G., McCandliss, S. R. & Moos, H. W. Potential variations in the interstellar N I abundance. *Astrophys. J.* **596,** L51–L54 (2003).
8. Le Petit, F., Roueff, E. & Herbst, E. H_3^+ and other species in the diffuse cloud towards ζ Persei: A new detailed model. *Astron. Astrophys.* **417,** 993–1002 (2004).
9. Walborn, N. R. The space distribution of the O stars in the solar neighborhood. *Astron. J.* **78,** 1067–1073 (1973).
10. Cruz-Gonzalez, C., Recillas-Cruz, E., Costero, R., Peimbert, M. & Torres-Peimbert, S. A catalogue of galactic O stars. The ionization of the low density interstellar medium by runaway stars. *Rev. Mex. Astron. Astrofis.* **1,** 211–259 (1974).
11. André, M. K. *et al.* Oxygen gas-phase abundance revisited. *Astrophys. J.* **591,** 1000–1012 (2003).
12. Perryman, M. A. C. *et al.* The *HIPPARCOS* catalogue. *Astron. Astrophys.* **323,** L49–L52 (1997).
13. Moos, H. W. *et al.* Overview of the *Far Ultraviolet Spectroscopic Explorer* mission. *Astrophys. J.* **538,** L1–L6 (2000).
14. Sahnow, D. J. *et al.* On-orbit performance of the *Far Ultraviolet Spectroscopic Explorer* satellite. *Astrophys. J.* **538,** L7–L11 (2000).
15. Dixon, W. V. & Sahnow, D. J. CalFUSE v2.2: An improved data calibration pipeline for the *Far Ultraviolet Spectroscopic Explorer* (*FUSE*) in astronomical data analysis software and systems XII. (Spec. Iss.; eds Payne, H.E., Jedrzejewski, R.I. & Hook, R. N.) *ASP Conf. Ser.* **295**, (2003) 241–244.
16. Knauth, D. C., Howk, J. C., Sembach, K. R., Lauroesch, J. T. & Meyer, D. M. On the origin of the high-ionization intermediate velocity gas toward HD 14434. *Astrophys. J.* **592,** 964–974 (2003).
17. Federman, S. R., Glassgold, A. E., Jenkins, E. B. & Shaya, E. J. The abundance of CO in diffuse interstellar clouds. An ultraviolet survey. *Astrophys. J.* **242,** 545–559 (1980).
18. Abgrall, H. & Roueff, E. Wavelengths, oscillator strengths and transition probabilities of the H_2 molecule for Lyman and Werner systems. *Astron. Astrophys.* (Suppl.) **79,** 313–328 (1989).
19. Abgrall, H., Roueff, E. & Viala, Y. Vibration-rotation transition probabilities for the ground electronic $X^1\Sigma^+$ state of HD. *Astron. Astrophys.* (Suppl.) **50,** 505–522 (1982).
20. Morton, D. C. Atomic data for resonance absorption lines. III. Wavelengths longward of the Lyman limit for the elements hydrogen to gallium. *Astrophys. J.* (Suppl.) **149,** 205–238 (2003).
21. Stark, G. *et al.* Line oscillator strength measurements in the 0–0 band of the $c_4'^1\Sigma_u^+ - X^1\Sigma_g^+$ transition of N_2. *Astrophys. J.* **531,** 321–328 (2000).
22. Conti, P. S. & Ebbets, D. Spectroscopic studies of O-type stars. VII. Rotational velocities *Vsini* and evidence for macroturbulent motions. *Astrophys. J.* **213,** 438–447 (1977).
23. Lanz, T. & Hubeny, T. A grid of non-LTE line-blanketed model atmospheres of O-type stars. *Astrophys. J.* (Suppl.) **146,** 417–441 (2003).
24. Sheffer, Y., Federman, S. R. & Andersson, B.-G. FUSE measurements of Rydberg bands of interstellar CO between 925 and 1150 Å. *Astrophys. J.* **597,** L29–L32 (2003).
25. Hedin, A. E. Extension of the MSIS thermospheric model into the middle and lower atmosphere. *J. Geophys. Res.* **96,** 1159–1172 (1991).
26. Clayton, R. N. Self shielding in the Solar Nebula. *Nature* **415,** 860–861 (2002).
27. Van Dishoeck, E. F. & Black, J. H. The photodissociation and chemistry of interstellar CO. *Astrophys. J.* **334,** 771–802 (1988).
28. Bohlin, R. C., Savage, B. D. & Drake, J. F. A survey of interstellar H I from L_α absorption measurements. II. *Astrophys. J.* **242,** 132–142 (1978).
29. Sneden, C., Gehrz, R. D., Hackwell, J. A., York, D. G. & Snow, T. P. Infrared colors and the diffuse interstellar bands. *Astrophys. J.* **223,** 168–179 (1978).

Supplementary Information accompanies the paper on **www.nature.com/nature**.

Acknowledgements We thank A. Fullerton, S. R. Federman, P. Feldman, E. B. Jenkins, P. Sonnentrucker and P. Wannier for discussions and G. Stark for sharing his unpublished N_2 *f*-values. This work is based on observations made with the NASA-CNES-CSA Far Ultraviolet Spectroscopic Explorer, which is operated for NASA by Johns Hopkins University.

Competing interests statement The authors declare that they have no competing financial interests.

Correspondence and requests for materials should be addressed to D.C.K. (dknauth@pha.jhu.edu).

A precision measurement of the mass of the top quark

DØ Collaboration*

**A list of authors and their affiliations appear at the end of the paper*

The standard model of particle physics contains parameters—such as particle masses—whose origins are still unknown and which cannot be predicted, but whose values are constrained through their interactions. In particular, the masses of the top quark (M_t) and *W* boson (M_W)[1] constrain the mass of the long-hypothesized, but thus far not observed, Higgs boson. A precise measurement of M_t can therefore indicate where to look for the Higgs, and indeed whether the hypothesis of a standard model Higgs is consistent with experimental data. As top quarks are produced in pairs and decay in only about 10^{-24} s into various final states, reconstructing their masses from their decay products is very challenging. Here we report a technique that extracts more information from each top-quark event and yields a greatly improved precision (of ± 5.3 GeV/c^2) when compared to previous measurements[2]. When our new result is combined with our published measurement in a complementary decay mode[3] and with the only other measurements available[2], the new world average for M_t becomes[4] 178.0 ± 4.3 GeV/c^2. As a

result, the most likely Higgs mass increases from the experimentally excluded[5] value[6] of 96 to 117 GeV/c^2, which is beyond current experimental sensitivity. The upper limit on the Higgs mass at the 95% confidence level is raised from 219 to 251 GeV/c^2.

The discovery of the top quark in 1995 served as one of the major confirmations of the validity of the standard model (SM)[7,8]. Of its many parameters, the mass of the top quark, in particular, reflects some of the most crucial aspects of the SM. This is because, in principle, the top quark is point-like and should be massless; yet, through its interactions with the hypothesized Higgs field, the physical mass of the top quark appears to be about the mass of a gold nucleus. Because it is so heavy, the top quark (along with the W boson) provides an unusually sensitive tool for investigating the Higgs field. M_W is known to a precision of 0.05%, while the uncertainty on M_t is at the 3% level[1]. Improvements in both measurements are required to restrict further the allowed range of mass for the Higgs; however, given the large uncertainty in M_t, an improvement in its precision is particularly important. As has been pointed out recently[9,10], a potential problem for the SM is that, on the basis of the currently accepted value for M_t, the most likely value of the Higgs mass[6] lies in a range that has already been excluded by experiment[5]. Precise knowledge of the Higgs mass is crucial for our understanding of the SM and any possible new physics beyond it. For example, in a large class of supersymmetric models (theoretically preferred solutions to the deficiencies of the SM), the Higgs mass has to be less than about 135 GeV/c^2. Although, unlike the SM, supersymmetry predicts more than one Higgs boson, the properties of the lightest one are expected to be essentially the same as those for the SM Higgs boson. Thus, if the SM-like Higgs is heavier than about 135 GeV/c^2, it would disfavour a large class of supersymmetric models. In addition, some of the current limits on supersymmetric particles from LEP[11] are extremely sensitive to M_t. In fact, for M_t greater than 179 GeV/c^2, the bounds on one of the major supersymmetry parameters, tanβ, which relates the properties of the SM-like Higgs boson and its heavier partners, would disappear completely[12]. Hence, in addition to the impact on searches for the Higgs boson, other important consequences call for improved precision on M_t, and this goal is the main subject of this paper.

The DØ experiment at the Fermilab Tevatron has studied a sample of $t\bar{t}$ events produced in proton–antiproton ($p\bar{p}$) interactions[13]. The total energy of 1.8 TeV released in a head-on collision of a 900-GeV p and a 900-GeV $\bar{p}$ is almost as large as the rest energy of ten gold nuclei. Each top (antitop) quark decays almost immediately into a bottom $b(\bar{b})$ quark and a W^+ (W^-) boson, and we have reexamined those events in which one of the W bosons decays into a charged lepton (electron or muon) and a neutrino, and the other W into a quark and an antiquark (see Fig. 1). These events and their selection criteria are identical to those used to extract the mass of the top quark in our previous publication, and correspond to an integrated luminosity of 125 events per pb. (That is, given the production cross-section of the $t\bar{t}$ in $p\bar{p}$ collisions at 1.8 TeV of 5.7 pb, as measured by DØ[14], these data correspond to approximately 700 produced $t\bar{t}$ pairs, a fraction of which is fully detected in various possible decay modes. Approximately 30% of these correspond to the lepton + jets topology categorized in Fig. 2, where 'jet' refers to products of the fragmentation of a quark into a collimated group of particles that are emitted along the quark's original direction.) The main background processes correspond to multijet production (20%), where one of the jets is reconstructed incorrectly as a lepton, and the W + jets production with leptonic W decays (80%), which has the same topology as the $t\bar{t}$ signal.

The previous DØ measurement of M_t in this lepton + jets channel is $M_t = 173.3 \pm 5.6$ (stat) ± 5.5 (syst) GeV/c^2, and is based on 91 candidate events. Information pertaining to the older analysis and the DØ detector can be found elsewhere[13,15].

The new method of M_t measurement is similar to one suggested previously (ref. 16 and references therein, and ref. 17) for $t\bar{t}$ dilepton decay channels (where both W bosons decay leptonically), and used in previous mass analyses of dilepton events[3], and akin to an approach suggested for the measurement of the mass of the W boson at LEP[18–20]. The critical differences from previous analyses in the lepton + jets decay channel lie in: (1) the assignment of more weight to events that are well measured or more likely to correspond to $t\bar{t}$ signal, and (2) the handling of the combinations of final-state objects (lepton, jets and imbalance in transverse momentum, the latter being a signature for an undetected neutrino) and their identification with top-quark decay products in an event (such as from ambiguity in choosing jets that correspond to b or $\bar{b}$ quarks from the decays of the t and $\bar{t}$ quarks). Also, because leading-order matrix elements were used to calculate the event weights, only events with exactly four jets are kept in this analysis, resulting in a candidate sample of 71 events. Although we are left with fewer events, the new method for extracting M_t provides substantial improvement in both statistical and systematic uncertainties.

We calculate as a function of M_t the differential probability that the measured variables in any event correspond to signal. The maximum of the product of these individual event probabilities provides the best estimate of M_t in the data sample. The impact of biases from imperfections in the detector and event-reconstruction algorithms is taken into account in two ways. Geometric acceptance, trigger efficiencies, event selection, and so on enter through a multiplicative acceptance function that is independent of M_t. Because the angular directions of all the objects in the event, as

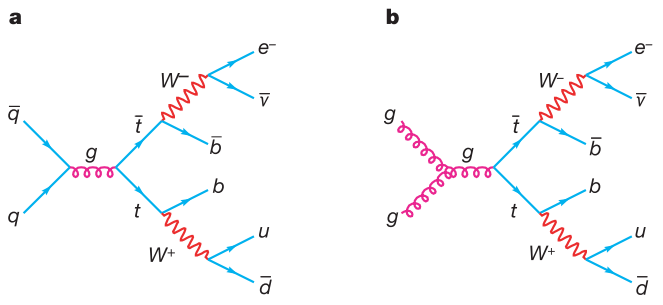

Figure 1 Feynman diagrams for $t\bar{t}$ production in $p\bar{p}$ collisions, with subsequent decays into an electron, neutrino, and quarks. Quark–antiquark production (**a**) is dominant, but gluon fusion (**b**) contributes ~10% to the cross-section. This particular final state ($e\bar{\nu}u\bar{d}b\bar{b}$) is one of the channels used in the analysis.

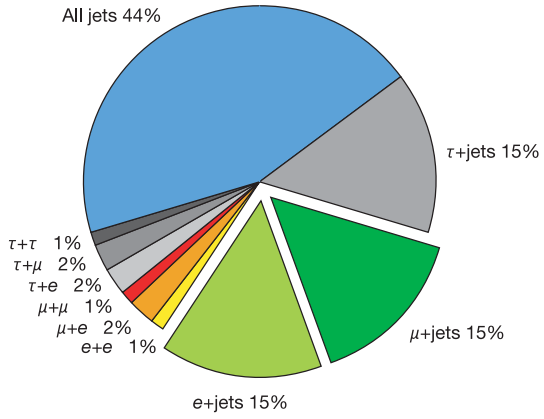

Figure 2 Relative importance of various $t\bar{t}$ decay modes. The 'lepton + jets' channel used in this analysis corresponds to the two offset slices of the pie-chart and amounts to 30% of all the $t\bar{t}$ decays.

well as the electron momentum, are measured with high precision, their measured values are used directly in the calculation of the probability that any event corresponds to $t\bar{t}$ or background production. The known momentum resolution is used to account for uncertainties in measurements of jet energies and muon momenta.

As in the previous analysis[13], momentum conservation in γ + jet events is used to check that the energies of jets in the experiment agree with Monte Carlo (MC) simulations. This calibration has an uncertainty $\delta E = (0.025E + 0.5\,\mathrm{GeV})$. Consequently, all jet energies in our sample are rescaled by $\pm\delta E$, the analysis redone, and half of the difference in the two rescaled results for M_t ($\delta M_t = 3.3\,\mathrm{GeV}/c^2$) is taken as a systematic uncertainty from this source. All other contributions to systematic uncertainty: MC modelling of signal ($\delta M_t = 1.1\,\mathrm{GeV}/c^2$) and background ($\delta M_t = 1.0\,\mathrm{GeV}/c^2$), effect of calorimeter noise and event pile-up ($\delta M_t = 1.3\,\mathrm{GeV}/c^2$), and other corrections from M_t extraction ($\delta M_t = 0.6\,\mathrm{GeV}/c^2$) are much smaller, and discussed in detail elsewhere[21,22]. It should be noted that the new mass measurement method provides a significant (about 40%, from ± 5.5 to $\pm 3.9\,\mathrm{GeV}/c^2$) reduction in systematic uncertainty, which is ultimately dominated by the measurement of jet energies. For details on the new analysis, see the Methods.

The final result is $M_t = 180.1 \pm 3.6$ (stat) ± 3.9 (syst) GeV/c^2. The improvement in statistical uncertainty over our previous measurement is equivalent to collecting a factor of 2.4 as much data. Combining the statistical and systematic uncertainties in quadrature, we obtain $M_t = 180.1 \pm 5.3\,\mathrm{GeV}/c^2$, which is consistent with our previous measurement in the same channel (at about 1.4 standard deviations), and has a precision comparable to all previous M_t measurements combined[1].

The new measurement can be combined with that obtained for the dilepton sample that was also collected at DØ during run I (ref. 3) ($M_t = 168.4 \pm 12.3$ (stat) ± 3.6 (syst) GeV/c^2), to yield the new DØ average for the mass of the top quark:

$$M_t = 179.0 \pm 5.1\,\mathrm{GeV}/c^2 \qquad (1)$$

Combining this with measurements from the CDF experiment[2] provides a new 'world average' (based on all measurements available) for the mass of the top quark[4]:

$$M_t = 178.0 \pm 4.3\,\mathrm{GeV}/c^2 \qquad (2)$$

dominated by our new measurement. This new world average shifts the best-fit value of the expected Higgs mass from 96 GeV/c^2 to 117 GeV/c^2 (see Fig. 3), which is now outside the experimentally excluded region, yet accessible in the current run of the Tevatron and at future runs at the Large Hadron Collider (LHC), at present under construction at CERN. (The upper limit on the Higgs mass at the 95% confidence level changes from 219 GeV/c^2 to 251 GeV/c^2.) Figure 3 shows the effect of using only the new DØ top mass for fits to the Higgs mass, and indicates a best value of 123 GeV/c^2 and the upper limit of 277 GeV/c^2 at the 95% confidence level. It should be noted that the horizontal scale in Fig. 3 is logarithmic, and the limits on the Higgs boson mass are therefore asymmetric.

The new method is already being applied to data being collected by the CDF and DØ experiments at the new run of the Fermilab Tevatron and should provide even higher precision on the determination of M_t, equivalent to more than a doubling of the data sample, relative to using the conventional method. An ultimate precision of about 2 GeV/c^2 on the mass of the top quark is expected to be reached in several years of Tevatron operation. Further improvement may eventually come from the LHC. □

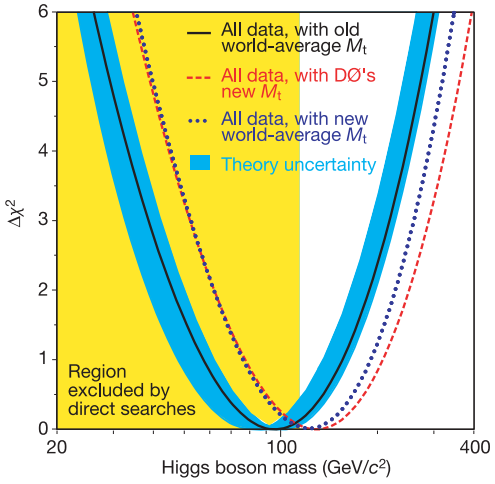

Figure 3 Current experimental constraints on the mass of the Higgs boson. The χ^2 for a global fit to electroweak data[6] is shown as a function of the Higgs mass. The solid line corresponds to the result for the previous world-averaged $M_t = 174.3 \pm 5.1\,\mathrm{GeV}/c^2$, with the blue band indicating the impact of theoretical uncertainty. The dotted line shows the result for the new world-averaged M_t of $178.0 \pm 4.3\,\mathrm{GeV}/c^2$, whereas the dashed line corresponds to using only the new DØ average of $179.0 \pm 5.1\,\mathrm{GeV}/c^2$. The yellow-shaded area on the left indicates the region of Higgs masses excluded by experiment (>114.4 GeV/c^2 at the 95% confidence level[5]). The improved M_t measurement shifts the most likely value of the Higgs mass above the experimentally excluded range.

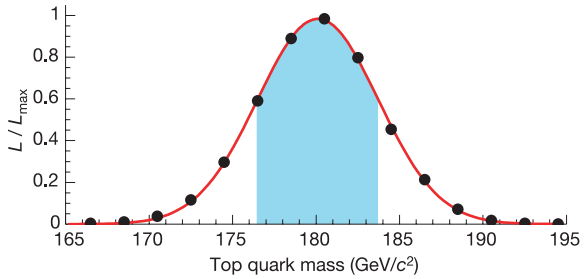

Figure 4 Determination of the mass of the top quark using the maximum-likelihood method. The points represent the likelihood of the fit used to extract M_t divided by its maximum value, as a function of M_t (after a correction for a $-0.5\,\mathrm{GeV}/c^2$ mass bias, see text). The solid line shows a gaussian fit to the points. The maximum likelihood corresponds to a mass of 180.1 GeV/c^2, which is the new DØ measurement of M_t in the lepton + jets channel. The shaded band corresponds to the range of ± 1 standard deviation, and indicates the $\pm 3.6\,\mathrm{GeV}/c^2$ statistical uncertainty of the fit.

Methods

The probability density as a function of M_t can be written as a convolution of the calculable cross-section and any effects from measurement resolution:

$$P(x, M_t) = \frac{1}{\sigma(M_t)} \int \mathrm{d}\sigma(y, M_t)\mathrm{d}q_1\,\mathrm{d}q_2 f(q_1) f(q_2) W(y, x) \qquad (3)$$

where $W(y, x)$, our general transfer function, is the normalized probability for the measured set of variables x to arise from a set of nascent (partonic) variables y, $\mathrm{d}\sigma(y, M_t)$ is the partonic theoretical differential cross-section, $f(q)$ are parton distribution functions that reflect the probability of finding any specific interacting quark (antiquark) with momentum q within the proton (antiproton), and $\sigma(M_t)$ is the total cross-section for producing $t\bar{t}$. The integral in equation (3) sums over all possible parton states, leading to what is observed in the detector.

The acceptance of the detector is given in terms of a function $A(x)$ that relates the probability $P_m(x, M_t)$ of measuring the observed variables x to their production probability $P(x, M_t)$: $P_m(x, M_t) = A(x)P(x, M_t)$. Effects from energy resolution, and so on are taken into account in the transfer function $W(y, x)$. The integrations in equation (3) over the eleven well-measured variables (three components of charged-lepton momentum and eight jet angles) and the four equations of energy-momentum conservation leave five integrals that must be performed to obtain the probability that any event represents $t\bar{t}$ (or background) production for some specified value of M_t.

The probability for a $t\bar{t}$ interpretation can be written as:

$$P_{t\bar{t}} = \frac{1}{12\sigma_{t\bar{t}}} \int \mathrm{d}^5\Omega \sum_{\mathrm{perm.},\nu} |\mathscr{M}_{t\bar{t}}|^2 \frac{f(q_1)f(q_2)}{|q_1||q_2|} \Phi_6 W_{\mathrm{jets}}(E_{\mathrm{part}}, E_{\mathrm{jet}})$$

where Ω represents a set of five integration variables, $\mathscr{M}_{t\bar{t}}$ is the leading-order matrix element for $t\bar{t}$ production[23,24], $f(q_1)$ and $f(q_2)$ are the CTEQ4M parton distribution functions for the incident quarks[25], Φ_6 is the phase-space factor for the six-object final state, and the sum is over all 12 permutations of the jets and all possible neutrino solutions.

$W_{\mathrm{jets}}(E_{\mathrm{part}}, E_{\mathrm{jet}})$ corresponds to a function that maps parton-level energies E_{part} to energies measured in the detector E_{jet} and is based on MC studies. A similar expression, using a matrix element for W + jets production (the dominant background source) that is independent of M_{t}, is used to calculate the probability for a background interpretation, P_{bkg}.

Studies of samples of HERWIG (ref. 26; we used version 5.1) MC events indicate that the new method is capable of providing almost a factor-of-two reduction in the statistical uncertainty on the extracted M_{t}. These studies also reveal that there is a systematic shift in the extracted M_{t} that depends on the amount of background there is in the data. To minimize this effect, a selection is introduced, based on the probability that an event represents background. The specific value of the P_{bkg} cut-off is based on MC studies carried out before applying the method to data, and, for $M_{\mathrm{t}} = 175\ \mathrm{GeV}/c^2$, retains 71% of the signal and 30% of the background. A total of 22 data events out of our 71 candidates pass this selection.

The final likelihood as a function of M_{t} is written as:

$$\ln L(M_{\mathrm{t}}) = \sum_{i=1}^{N} \ln[c_1 P_{t\bar{t}}(x_i, M_{\mathrm{t}}) + c_2 P_{\mathrm{bkg}}(x_i)] - N \int A(x)[c_1 P_{t\bar{t}}(x, M_{\mathrm{t}}) + c_2 P_{\mathrm{bkg}}(x)]\mathrm{d}x$$

The integration is performed using MC methods. The best value of M_{t} (when L is at its maximum L_{max}) represents the most likely mass of the top quark in the final N-event sample, and the parameters c_i reflect the amounts of signal and background. MC studies show that there is a downward shift of $0.5\ \mathrm{GeV}/c^2$ in the extracted mass, and this correction is applied to the result. Reasonable changes in the cut-off on P_{bkg} do not have a significant impact on M_{t}.

Figure 4 shows the value of $L(M_{\mathrm{t}})/L_{\mathrm{max}}$ as a function of M_{t} for the 22 events that pass all selection criteria, after correction for the $0.5\ \mathrm{GeV}/c^2$ bias in mass. The likelihood is maximized with respect to the parameters c_i at each mass point. The gaussian fit in the figure yields $M_{\mathrm{t}} = 180.1\ \mathrm{GeV}/c^2$, with a statistical uncertainty of $\delta M_{\mathrm{t}} = 3.6\ \mathrm{GeV}/c^2$. The systematic uncertainty, dominated by the measurement of jet energies, as discussed above, amounts to $\delta M_{\mathrm{t}} = 3.9\ \mathrm{GeV}/c^2$. When added in quadrature to the statistical uncertainty from the fit, it yields the overall uncertainty on the new M_{t} measurement of $\pm 5.3\ \mathrm{GeV}/c^2$.

Received 23 January; accepted 21 April 2004; doi:10.1038/nature02589.

1. Hagiwara, K. *et al.* Review of particle physics. *Phys. Rev. D* **66,** 010001 (2002).
2. Affolder, T. *et al.* (CDF Collaboration). Measurement of the top quark mass with the Collider Detector at Fermilab. *Phys. Rev. D* **63,** 032003 (2001).
3. Abbott, B. *et al.* (DØ Collaboration). Measurement of the top quark mass in the dilepton channel. *Phys. Rev. D* **60,** 052001 (1999).
4. The CDF Collaboration, the DØ Collaboration, and the TEVATRON Electro-Weak Working Group. Combination of CDF and DØ Results on the Top-Quark Mass. Preprint at http://www.arXiv.org/hep-ex/0404010 (2004).
5. Barate, R. *et al.* (ALEPH Collaboration, DELPHI Collaboration, L3 Collaboration, OPAL Collaboration, and LEP Working Group for Higgs boson searches). Search for the standard model Higgs boson at LEP. *Phys. Lett. B* **565,** 61–75 (2003).
6. The LEP Collaborations ALEPH, DELPHI, L3, and OPAL, the LEP Electroweak Working Group, and the SLD Heavy Flavour Group. A combination of preliminary electroweak measurements and constraints on the standard model. Preprint at http://www.arXiv.org/hep-ex/0312023 (2003).
7. Abe, F. *et al.* (CDF Collaboration). Observation of top quark production in $p\bar{p}$ collisions with the Collider Detector at Fermilab. *Phys. Rev. Lett.* **74,** 2626–2631 (1995).
8. Abachi, S. *et al.* (DØ Collaboration). Observation of the top quark. *Phys. Rev. Lett.* **74,** 2632–2637 (1995).
9. Ellis, J. The 115 GeV Higgs odyssey. *Comments Nucl. Part. Phys. A* **2,** 89–103 (2002).
10. Chanowitz, M. S. Electroweak data and the Higgs boson mass: a case for new physics. *Phys. Rev. D* **66,** 073002 (2002).
11. The LEP Collaborations ALEPH, DELPHI, L3 & OPAL, the LEP Higgs Working Group. Searches for the neutral Higgs bosons of the MSSM: preliminary combined results using LEP data collected at energies up to 209 GeV. Preprint at http://www.arXiv.org/hep-ex/0107030 (2001).
12. Degrassi, G., Heinemeyer, S., Hollik, W., Slavich, P. & Weiglein, G. Towards high-precision predictions for the MSSM Higgs sector. *Eur. Phys. J. C* **28,** 133–143 (2003).
13. Abbott, B. *et al.* (DØ Collaboration). Direct measurement of the top quark mass by the DØ collaboration. *Phys. Rev. D* **58,** 052001 (1998).
14. Abazov, V. M. *et al.* (DØ Collaboration). $t\bar{t}$ production cross section in $p\bar{p}$ collisions at $\sqrt{s} = 1.8$ TeV. *Phys. Rev. D* **67,** 012004 (2003).
15. Abachi, S. *et al.* (DØ Collaboration). The DØ detector. *Nucl. Instrum. Methods A* **338,** 185–253 (1994).
16. Dalitz, R. H. & Goldstein, G. R. Test of analysis method for top–antitop production and decay events. *Proc. R. Soc. Lond. A* **445,** 2803–2834 (1999).
17. Kondo, K. *et al.* Dynamical likelihood method for reconstruction of events with missing momentum. 3: Analysis of a CDF high p_T $e\mu$ event as $t\bar{t}$ production. *J. Phys. Soc. Jpn* **62,** 1177–1182 (1993).
18. Berends, F. A., Papadopoulos, C. G. & Pittau, R. On the determination of M_W and TGCs in W-pair production using the best measured kinematical variables. *Phys. Lett. B* **417,** 385–389 (1998).
19. Abreu, P. *et al.* (DELPHI Collaboration). Measurement of the W pair cross-section and of the W Mass in e^+e^- interactions at 172 GeV. *Eur. Phys. J. C* **2,** 581–595 (1998).
20. Juste, A. Measurement of the W mass in e^+e^- annihilation PhD thesis, 1–160, Univ. Autonoma de Barcelona (1998).
21. Estrada, J. Maximal use of kinematic information for extracting the top quark mass in single-lepton $t\bar{t}$ events PhD thesis, 1–132, Univ. Rochester (2001).
22. Canelli, F. Helicity of the W boson in single-lepton $t\bar{t}$ events PhD thesis. 1–241, Univ. Rochester (2003).
23. Mahlon, G. & Parke, S. Angular correlations in top quark pair production and decay at hadron colliders. *Phys. Rev. D* **53,** 4886–4896 (1996).
24. Mahlon, G. & Parke, S. Maximizing spin correlations in top quark pair production at the Tevatron. *Phys. Lett. B* **411,** 173–179 (1997).
25. Lai, H. L. *et al.* (CTEQ Collaboration). Global QCD analysis and the CTEQ parton distributions. *Phys. Rev. D* **51,** 4763–4782 (1995).
26. Marchesini, G. *et al.* HERWIG: a Monte Carlo event generator for simulating hadron emission reactions with interfering gluons. *Comput. Phys. Commun.* **67,** 465–508 (1992).

Acknowledgements We are grateful to our colleagues A. Quadt and M. Mulders for reading of the manuscript and comments. We thank the staffs at Fermilab and collaborating institutions, and acknowledge support from the Department of Energy and National Science Foundation (USA), Commissariat à L'Energie Atomique and CNRS/Institut National de Physique Nucléaire et de Physique des Particules (France), Ministry for Science and Technology and Ministry for Atomic Energy (Russia), CAPES, CNPq and FAPERJ (Brazil), Departments of Atomic Energy and Science and Education (India), Colciencias (Colombia), CONACyT (Mexico), Ministry of Education and KOSEF (Korea), CONICET and UBACyT (Argentina), The Foundation for Fundamental Research on Matter (The Netherlands), PPARC (UK), Ministry of Education (Czech Republic), the A. P. Sloan Foundation, and the Research Corporation.

Authors' contributions We wish to note the great number of contributions made by the late Harry Melanson to the DØ experiment, through his steady and inspirational leadership of the physics, reconstruction and algorithm efforts.

Competing interests statement The authors declare that they have no competing financial interests.

Correspondence and requests for materials should be addressed to J. Estrada (estrada@fnal.gov).

DØ Collaboration (Participants are listed in alphabetical order.)

V. M. Abazov[1], B. Abbott[2], A. Abdesselam[3], M. Abolins[4], V. Abramov[5], B. S. Acharya[6], D. L. Adams[7], M. Adams[8], S. N. Ahmed[9], G. D. Alexeev[1], A. Alton[10], G. A. Alves[11], Y. Arnoud[12], C. Avila[13], V. V. Babintsev[5], L. Babukhadia[14], T. C. Bacon[15], A. Baden[16], S. Baffioni[17], B. Baldin[18], P. W. Balm[19], S. Banerjee[6], E. Barberis[20], P. Baringer[21], J. Barreto[11], J. F. Bartlett[18], U. Bassler[22], D. Bauer[23], A. Bean[21], F. Beaudette[3], M. Begel[24], A. Belyaev[25], S. B. Beri[26], G. Bernardi[22], I. Bertram[27], A. Besson[12], R. Beuselinck[15], V. A. Bezzubov[5], P. C. Bhat[18], V. Bhatnagar[26], M. Bhattacharjee[14], G. Blazey[28], F. Blekman[19], S. Blessing[25], A. Boehnlein[18], N. I. Bojko[5], T. A. Bolton[29], F. Borcherding[18], K. Bos[19], T. Bose[30], A. Brandt[31], G. Briskin[32], R. Brock[4], G. Brooijmans[30], A. Bross[18], D. Buchholz[33], M. Buehler[8], V. Buescher[34], V. S. Burtovoi[5], J. M. Butler[35], F. Canelli[24], W. Carvalho[36], D. Casey[4], H. Castilla-Valdez[37], D. Chakraborty[28], K. M. Chan[24], S. V. Chekulaev[5], D. K. Cho[24], S. Choi[38], S. Chopra[7], D. Claes[39], A. R. Clark[40], B. Connolly[25], W. E. Cooper[18], D. Coppage[21], S. Crépé-Renaudin[12], M. A. C. Cummings[28], D. Cutts[32], H. da Motta[11], G. A. Davis[24], K. De[31], S. J. de Jong[9], M. Demarteau[18], R. Demina[24], P. Demine[41], D. Denisov[18], S. P. Denisov[5], S. Desai[14], H. T. Diehl[18], M. Diesburg[18], S. Doulas[20], L. V. Dudko[42], L. Duflot[3], S. R. Dugad[6], A. Duperrin[17], A. Dyshkant[28], D. Edmunds[4], J. Ellison[38], J. T. Eltzroth[31], V. D. Elvira[18], R. Engelmann[14], S. Eno[16], G. Eppley[43], P. Ermolov[42], O. V. Eroshin[5], J. Estrada[24], H. Evans[30], V. N. Evdokimov[5], T. Ferbel[24], F. Filthaut[9], H. E. Fisk[18], M. Fortner[28], H. Fox[33], S. Fu[30], S. Fuess[18], E. Gallas[18], A. N. Galyaev[5], M. Gao[30], V. Gavrilov[44], R. J. Genik II[27], K. Genser[18], C. E. Gerber[8], Y. Gershtein[32], G. Ginther[24], B. Gómez[13], P. I. Goncharov[5], K. Gounder[18], A. Goussiou[45], P. D. Grannis[14], H. Greenlee[18], Z. D. Greenwood[46], S. Grinstein[47], L. Groer[30], S. Grünendahl[18], M. W. Grünewald[48], S. N. Gurzhiev[5], G. Gutierrez[18], P. Gutierrez[2], N. J. Hadley[16], H. Haggerty[18], S. Hagopian[25], V. Hagopian[25], R. E. Hall[49], C. Han[10], S. Hansen[18], J. M. Hauptman[50], C. Hebert[21], D. Hedin[28], J. M. Heinmiller[8], A. P. Heinson[38], U. Heintz[35], M. D. Hildreth[45], R. Hirosky[51], J. D. Hobbs[14], B. Hoeneisen[52], J. Huang[23], Y. Huang[10], I. Iashvili[38], R. Illingworth[15], A. S. Ito[18], M. Jaffré[3], S. Jain[2], R. Jesik[15], K. Johns[53], M. Johnson[18], A. Jonckheere[18], H. Jöstlein[18], A. Juste[18], W. Kahl[29], S. Kahn[7], E. Kajfasz[17], A. M. Kalinin[1], D. Karmanov[42], D. Karmgard[45], R. Kehoe[4], S. Kesisoglou[32], A. Khanov[24], A. Kharchilava[45], B. Klima[18], J. M. Kohli[26], A. V. Kostritskiy[5], J. Kotcher[7], B. Kothari[30], A. V. Kozelov[5], E. A. Kozlovsky[5], J. Krane[50], M. R. Krishnaswamy[6], P. Krivkova[54], S. Krzywdzinski[18], M. Kubantsev[29], S. Kuleshov[44], Y. Kulik[18], S. Kunori[16], A. Kupco[55], V. E. Kuznetsov[38], G. Landsberg[32], W. M. Lee[25], A. Leflat[42], F. Lehner[18]*, C. Leonidopoulos[30], J. Li[31], Q. Z. Li[18], J. G. R. Lima[28], D. Lincoln[18], S. L. Linn[25], J. Linnemann[4], R. Lipton[18], A. Lucotte[12], L. Lueking[18], C. Lundstedt[39], C. Luo[23], A. K. A. Maciel[28], R. J. Madaras[40], V. L. Malyshev[1], V. Manankov[42], H. S. Mao[56], T. Marshall[23], M. I. Martin[28], S. E. K. Mattingly[32], A. A. Mayorov[5], R. McCarthy[14], T. McMahon[57], H. L. Melanson[18], A. Melnitchouk[32], A. Merkin[42], K. W. Merritt[18], C. Miao[32], H. Miettinen[43], D. Mihalcea[28], N. Mokhov[18], N. K. Mondal[6], H. E. Montgomery[18], R. W. Moore[4], Y. D. Mutaf[14], E. Nagy[17], M. Narain[35], V. S. Narasimham[6], N. A. Naumann[9], H. A. Neal[10], J. P. Negret[13], S. Nelson[25], A. Nomerotski[18], T. Nunnemann[18], D. O'Neil[4], V. Oguri[36], N. Oshima[18], P. Padley[43], K. Papageorgiou[8], N. Parashar[46],

R. Partridge[32], N. Parua[14], A. Patwa[14], O. Peters[19], P. Pétroff[3], R. Piegaia[47], B. G. Pope[4], H. B. Prosper[25], S. Protopopescu[7], M. B. Przybycien[33]*, J. Qian[10], S. Rajagopalan[7], P. A. Rapidis[18], N. W. Reay[29], S. Reucroft[20], M. Ridel[3], M. Rijssenbeek[14], F. Rizatdinova[29], T. Rockwell[4], C. Royon[41], P. Rubinov[18], R. Ruchti[45], B. M. Sabirov[1], G. Sajot[12], A. Santoro[36], L. Sawyer[46], R. D. Schamberger[14], H. Schellman[33], A. Schwartzman[47], E. Shabalina[8], R. K. Shivpuri[58], D. Shpakov[20], M. Shupe[53], R. A. Sidwell[29], V. Simak[55], V. Sirotenko[18], P. Slattery[24], R. P. Smith[18], G. R. Snow[39], J. Snow[57], S. Snyder[7], J. Solomon[8], Y. Song[31], V. Sorín[47], M. Sosebee[31], N. Sotnikova[42], K. Soustruznik[54], M. Souza[11], N. R. Stanton[29], G. Steinbrück[30], D. Stoker[59], V. Stolin[44], A. Stone[8], D. A. Stoyanova[5], M. A. Strang[31], M. Strauss[2], M. Strovink[40], L. Stutte[18], A. Sznajder[36], M. Talby[17], W. Taylor[14], S. Tentindo-Repond[25], T. G. Trippe[40], A. S. Turcot[7], P. M. Tuts[30], R. Van Kooten[23], V. Vaniev[5], N. Varelas[8], F. Villeneuve-Seguier[17], A. A. Volkov[5], A. P. Vorobiev[5], H. D. Wahl[25], Z.-M. Wang[14], J. Warchol[45], G. Watts[60], M. Wayne[45], H. Weerts[4], A. White[31], D. Whiteson[40], D. A. Wijngaarden[9], S. Willis[28], S. J. Wimpenny[38], J. Womersley[18], D. R. Wood[20], Q. Xu[10], R. Yamada[18], T. Yasuda[18], Y. A. Yatsunenko[1], K. Yip[7], J. Yu[31], M. Zanabria[13], X. Zhang[2], B. Zhou[10], Z. Zhou[50], M. Zielinski[24], D. Zieminska[23], A. Zieminski[23], V. Zutshi[28], E. G. Zverev[42] & A. Zylberstejn[41]

Affiliations for participants: 1, Joint Institute for Nuclear Research, P O Box 79, 141980 Dubna, Russia; 2, University of Oklahoma, Department of Physics and Astronomy, Norman, Oklahoma 73019, USA; 3, Laboratoire de l'Accélérateur Linéaire, IN2P3-CNRS, BP 34, Batiment 200, F-91898 Orsay, France; 4, Michigan State University, Department of Physics and Astronomy, East Lansing, Michigan 48824, USA; 5, Institute for High Energy Physics, 142284 Protvino, Russia; 6, Tata Institute of Fundamental Research, School of Natural Sciences, Homi Bhabha Rd, Mumbai 400005, India; 7, Brookhaven National Laboratory, Physics Department, Bldg 510C, Upton, New York 11973, USA; 8, University of Illinois at Chicago, Department of Physics, 845 W. Taylor, Chicago, Illinois 60607, USA; 9, University of Nijmegen/NIKHEF, P O Box 9010, NL-6500 GL Nijmegen, The Netherlands; 10, University of Michigan, Department of Physics, 500 E. University Avenue, Ann Arbor, Michigan 48109, USA; 11, LAFEX, Centro Brasileiro de Pesquisas Físicas, Rua Dr Xavier Sigaud, 150, 22290-180 Rio de Janeiro, Brazil; 12, Laboratoire de Physique Subatomique et de Cosmologie, IN2P3-CNRS, Université de Grenoble 1, 53 Avenue des Martyrs, F-38026 Grenoble, France; 13, Universidad de los Andes, Department de Fisica, HEP Group, Apartado Aereo 4976, Bogotá, Colombia; 14, State University of New York, Department of Physics and Astronomy, Stony Brook, New York 11794, USA; 15, Imperial College London, Department of Physics, Prince Consort Road, London SW7 2BW, UK; 16, University of Maryland, Department of Physics, College Park, Maryland 20742, USA; 17, CPPM, IN2P3-CNRS, Université de la Méditerranée, 163 Avenue de Luminy, F-13288 Marseille, France; 18, Fermi National Accelerator Laboratory, P O Box 500, Batavia, Illinois 60510, USA; 19, FOM-Institute NIKHEF and University of Amsterdam/NIKHEF, P O Box 41882, 1009 DB Amsterdam, The Netherlands; 20, Northeastern University, Department of Physics, Boston, Massachusetts 02115, USA; 21, University of Kansas, Department of Physics and Astronomy, 1251 Wescoe Hall Drive, Lawrence, Kansas 66045, USA; 22, LPNHE, Universités Paris VI and VII, IN2P3-CNRS, 4 Place Jussieu, Tour 33, F-75252 Paris, France; 23, Indiana University, Department of Physics, 727 E. 3rd St, Bloomington, Indiana 47405, USA; 24, University of Rochester, Department of Physics and Astronomy, Rochester, New York 14627, USA; 25, Florida State University, Department of Physics 4350, Tallahassee, Florida 32306, USA; 26, Panjab University, Department of Physics, Chandigarh 160014, India; 27, Lancaster University, Department of Physics, Lancaster LA1 4YB, United Kingdom; 28, Northern Illinois University, Department of Physics, DeKalb, Illinois 60115, USA; 29, Kansas State University, Department of Physics, Manhattan, Kansas 66506, USA; 30, Columbia University, Department of Physics, 538 W. 120th St, New York, New York 10027, USA; 31, University of Texas, Department of Physics, Box 19059, Arlington, Texas 76019, USA; 32, Brown University, Department of Physics, 182 Hope St, Providence, Rhode Island 02912, USA; 33, Northwestern University, Department of Physics and Astronomy, 2145 Sheridan Road, Evanston, Illinois 60208, USA; 34, Universität Freiburg, Physikalisches Institut, Hermann-Herder-Strasse 3, 79104 Freiburg, Germany; 35, Boston University, Department of Physics, 590 Commonwealth Avenue, Boston, Massachusetts 02215, USA; 36, Universidade do Estado do Rio de Janeiro, Instituto de Física, Rua São Francisco Xavier, 524, 20559-900 Rio de Janeiro, Brazil; 37, CINVESTAV, Departamento de Física, P O Box 14-740, 07000 Mexico City, Mexico; 38, University of California, Department of Physics, Riverside, California 92521, USA; 39, University of Nebraska, Department of Physics and Astronomy, Lincoln, Nebraska 68588, USA; 40, Lawrence Berkeley National Laboratory and University of California, 1 Cyclotron Road, Berkeley, California 94720, USA; 41, DAPNIA/Service de Physique des Particules, CEA, Saclay, F-91191 Gif-sur-Yvette, France; 42, Moscow State University, Department of Physics, Vorobjovy Gory, 119899 Moscow, Russia; 43, Rice University, Bonner Nuclear Lab, P O Box 1892, Houston, Texas 77005, USA; 44, Institute for Theoretical and Experimental Physics, B. Cheremushkinskaya ul. 25, 117259 Moscow, Russia; 45, University of Notre Dame, Department of Physics, Notre Dame, Indiana 46556, USA; 46, Louisiana Tech University, Department of Physics, Ruston, Louisiana 71272, USA; 47, Universidad de Buenos Aires, Departamento de Física, FCEN, Pabellón 1, Ciudad Universitaria, 1428 Buenos Aires, Argentina; 48, University College Dublin, Department of Experimental Physics, Faculty of Science, Belfield, Dublin 4, Ireland; 49, California State University, Department of Physics, 2345 E. San Ramon Avenue, Fresno, California 93740, USA; 50, Iowa State University, Department of Physics, High Energy Physics Group, Ames, Iowa 50011, USA; 51, University of Virginia, Department of Physics, Charlottesville, Virginia 22901, USA; 52, Universidad San Francisco de Quito, P O Box 17-12-841, Quito, Ecuador; 53, University of Arizona, Department of Physics, P O Box 210081, Tucson, Arizona 85721, USA; 54, Institute of Particle and Nuclear Physics, Center for Particle Physics, Faculty of Mathematics and Physics, Charles University in Prague, V Holesovickach 2, CZ-18000 Prague 8, Czech Republic; 55, Institute of Physics of the Academy of Sciences of the Czech Republic, Center for Particle Physics, Na Slovance 2, CZ-18221 Prague 8, Czech Republic; 56, Institute of High Energy Physics, P O Box 918, Beijing 100039, China; 57, Langston University, Department of Mathematics, Langston, Oklahoma 73050, USA; 58, Delhi University, Department of Physics and Astrophysics, Delhi 110007, India; 59, University of California, Department of Physics and Astronomy, 4129 Frederick Reines Hall, Irvine, California 92697, USA; 60, University of Washington, Department of Physics, P O Box 351560, Seattle, Washington 98195, USA.

*Present addresses: University of Zurich, Zurich, Switzerland (F.L.); Institute of Nuclear Physics, Krakow, Poland (M.B.P.)

Energy-transfer pumping of semiconductor nanocrystals using an epitaxial quantum well

Marc Achermann[1], Melissa A. Petruska[1], Simon Kos[1], Darryl L. Smith[1], Daniel D. Koleske[2] & Victor I. Klimov[1]

[1]*Los Alamos National Laboratory, Los Alamos, New Mexico 87545, USA*
[2]*Sandia National Laboratories, Albuquerque, New Mexico 87185, USA*

As a result of quantum-confinement effects, the emission colour of semiconductor nanocrystals can be modified dramatically by simply changing their size[1,2]. Such spectral tunability, together with large photoluminescence quantum yields and high photostability, make nanocrystals attractive for use in a variety of light-emitting technologies—for example, displays, fluorescence tagging[3], solid-state lighting and lasers[4]. An important limitation for such applications, however, is the difficulty of achieving electrical pumping, largely due to the presence of an insulating organic capping layer on the nanocrystals. Here, we describe an approach for indirect injection of electron–hole pairs (the electron–hole radiative recombination gives rise to light emission) into nanocrystals by non-contact, non-radiative energy transfer from a proximal quantum well that can in principle be pumped either electrically or optically. Our theoretical and experimental results indicate that this transfer is fast enough to compete with electron–hole recombination in the quantum well, and results in greater than 50 per cent energy-transfer efficiencies in the tested structures. Furthermore, the measured energy-transfer rates are sufficiently large to provide pumping in the stimulated emission regime, indicating the feasibility of nanocrystal-based optical amplifiers and lasers based on this approach.